The Plant Cell, Vol. 11, 2123–2137, November 1999, www.plantcell.org © 1999 American Society of Plant Physiologists

Genetic Regulation of Vascular Tissue Patterning in Arabidopsis

Francine M. Carland,[a,1] Barbara L. Berg,[b,1,2] Jonathan N. FitzGerald,[b] Suchaya Jinamornphongs,[b] Timothy Nelson,[a] and Brian Keith[c,3,4]

[a] Department of Molecular, Cellular, and Developmental Biology, Yale University, New Haven, Connecticut 06520-8104
[b] Department of Molecular Genetics and Cell Biology, University of Chicago, 1103 East 57th Street, Chicago, Illinois 60637
[c] Department of Medicine, University of Chicago, 5841 Maryland Avenue, Chicago, Illinois 60637

Plants transport water and nutrients through a complex vascular network comprised of interconnected, specialized cell types organized in discrete bundles. To identify genetic determinants of vascular tissue patterning, we conducted a screen for mutants with altered vascular bundle organization in Arabidopsis cotyledons. Mutations in two genes, *CVP1* and *CVP2* (for cotyledon vascular pattern), specifically disrupt the normal pattern of vascular bundles in cotyledons, mature leaves, and inflorescence stems. The spatial distribution of the procambium, the precursor to mature vascular tissue, is altered in *cvp1* and *cvp2* embryos, suggesting that *CVP1* and *CVP2* act at a very early step in vascular patterning. Similarly, in developing stems of *cvp1* and leaves of *cvp2*, the pattern of vascular differentiation is defective, but the maturation of individual vascular cells appears to be normal. There are no discernible alterations in cell morphology in *cvp2* mutants. In contrast, *cvp1* mutants are defective in directional orientation of the provascular strand, resulting in a failure to establish uniformly aligned vascular cells, and they also show a reduction in vascular cell elongation. Neither *cvp1* nor *cvp2* mutants displayed altered auxin perception, biosynthesis, or transport, suggesting that auxin metabolism is not generally affected in these mutants.

INTRODUCTION

The development of a complex vascular network that transports water, minerals, photosynthate, and signal molecules is essential to plants growing in nonaquatic environments. The positional signals that specify vascular cell identity, and thereby generate this network, are currently unknown. However, the species-specific patterns of vascular tissues in plant tissues suggest that their spatial distribution is subject to genetic regulation.

Vascular systems in most plants are comprised of several distinct cell and tissue types, including xylem and phloem, which are primarily responsible for transporting water and organic compounds, respectively. These tissues differentiate as strands of elongated cells, which are connected end to end through specialized cell wall structures (Esau, 1965; Raven et al., 1976). Xylem and phloem are organized in bundles with associated supporting cell types, including companion cells, sclerenchyma, and vascular parenchyma (Esau, 1965). These vascular bundles are connected to form an integrated network that connects all parts of the plant (Steeves and Sussex, 1989). The earliest observable stage in the differentiation of primary vascular tissues is the appearance of procambium, a meristematic tissue consisting of elongated, cytoplasmically dense cells (Esau, 1965). Procambial strands in immature shoot and root tissue can be traced in histological sections into mature, differentiated vascular bundles, indicating that procambium is the precursor to mature vascular tissue (Raven et al., 1976; Steeves and Sussex, 1989).

The molecular signals that induce the formation of the procambium in particular spatial patterns are not known. Clonal analysis of chimeric markers in several plant species has demonstrated that cell fate in plants is determined primarily by position and relies little on cell lineage (Poethig et al., 1986; Jegla and Sussex, 1989; Dawe and Freeling, 1991). The establishment of a complex vascular system offers a particularly striking example of the precision with which these positional signals must be controlled, because plant cells do not migrate relative to each other during development. In particular, the differentiation of a file of xylem cells requires their complete cellular autolysis, producing an empty conduit of dead cells with reinforced, lignified cell walls through which water flows under the force of transpiration (Esau, 1965; Steeves and Sussex, 1989). Characterizing the molecular mechanisms by which particular files of cells perceive

[1] These authors contributed equally to this work.
[2] Current address: Frederick Hutchinson Cancer Research Center, Seattle, WA 98109.
[3] Current address: Abramson Cancer Research Institute, 477 BRB II/III, University of Pennsylvania, Philadelphia, PA 19104.
[4] To whom correspondence should be addressed. E-mail bkeith@mail.med.upenn.edu; fax 215-746-5511.

inductive signals that trigger this apoptotic terminal differentiation (whereas adjacent cells remain viable and take on other cellular fates) is of both basic and applied biological interest, because plant vascular tissues are the major components of wood and plant-derived fiber (Raven et al., 1976).

Previous studies on vascular differentiation and patterning in plants have focused primarily on the effects of the growth regulator auxin (indole-3-acetic acid [IAA]; Aloni, 1987; Fukuda, 1992; Northcote, 1995; Nelson and Dengler, 1997). For example, auxin has been shown to stimulate the differentiation of isolated *Zinnia* leaf protoplasts into definitive xylem tracheary elements in vitro (Fukuda, 1992). In addition, exogenous auxin can induce existing parenchyma cells to redifferentiate into new vascular bundles in wounded bean and pea stems (Sachs, 1991a). Overproduction of auxin also leads to increased production of vascular tissue in transgenic plants, whereas auxin inactivation decreases vascular tissue differentiation (Klee et al., 1987; Romano et al., 1991). A variety of surgical experiments has led to a model proposing that vascular bundles differentiate from files of cells that transport auxin efficiently from sources to sinks, and that genetic prepatterning plays little, if any role (Sachs, 1991b; see Discussion). In fact, Arabidopsis mutants defective in auxin transport display altered vascular differentiation and patterning, although these mutations are pleiotropic and affect many different tissues (Okada et al., 1991; Carland and McHale, 1996; Przemeck et al., 1996). Although these studies clearly indicate a role for auxin in vascular tissue differentiation, it has not been demonstrated that stochastic auxin transport is the sole determinant of vascular tissue patterns during normal development.

To investigate the extent of genetic regulation in vascular patterning in plants, we conducted a screen to identify Arabidopsis mutants specifically altered in this process. Here, we describe the identification, phenotypes, and genetic interactions of mutations in two genes that disrupt vascular bundle patterns in cotyledons, leaves, and inflorescence stems. The *cvp* (for cotyledon vascular pattern) mutants clearly possess altered vascular bundle patterns, yet their overall morphology appears essentially normal, and they display wild-type levels of free IAA, basipetal auxin transport, and sensitivity to exogenous auxin. These results suggest that the *cvp* mutants are defective in processes highly specific to vascular patterning. Moreover, *cvp1* and *cvp2* disrupt the distribution of procambial tissue as early as in embryonic cotyledons, suggesting that both genes act at a very early step in vascular patterning and differentiation.

RESULTS

Genetic Screen for Vascular Pattern Mutants

Cotyledons (embryonic leaves) from 7-day-old seedlings were viewed under a dissecting microscope to identify vascular patterning mutants. Cotyledons develop during embryogenesis as storage organs for early postgerminative growth and offer several powerful advantages for observing vascular defects: (1) the vascular pattern in cotyledons is simple and relatively constant; and (2) several developmental events that occur simultaneously in true leaf development are separated temporally in cotyledon development (Tsukaya et al., 1994). Specifically, procambial tissues are formed during embryogenesis, whereas final differentiation of vascular tissue cell types occurs after germination (Dharmawardhana et al., 1992). In contrast, both processes occur simultaneously in different regions of developing true leaves (Esau, 1965).

To establish clearly the range of wild-type vascular patterns, we examined single excised fully expanded cotyledons from 272 Arabidopsis seedlings (ecotype Columbia). As shown in Figure 1, lignified xylem strands were clearly visible in whole-mount preparations (see Methods). The vascular pattern observed in wild-type cotyledons (Figure 1A) was strikingly similar, with four loops of xylem strands emanating from a midvein (242 of 272). In many cases, one or both strands comprising the two proximal loops appeared unconnected to the base of the midvein (157 of 242). A few cotyledons had two (nine of 272), three (20 of 272), or five (one of 272) "closed" loops. Given this small degree of variability, the wild-type cotyledon vascular pattern was defined conservatively as consisting of at least two closed loops of xylem strands.

To identify mutants, we dissected and examined single cotyledons from 34,040 seedlings from 10 different M_2 pools for altered xylem strand patterns. Putative mutants (209) were transferred to soil and allowed to self-fertilize. M_3 prog-

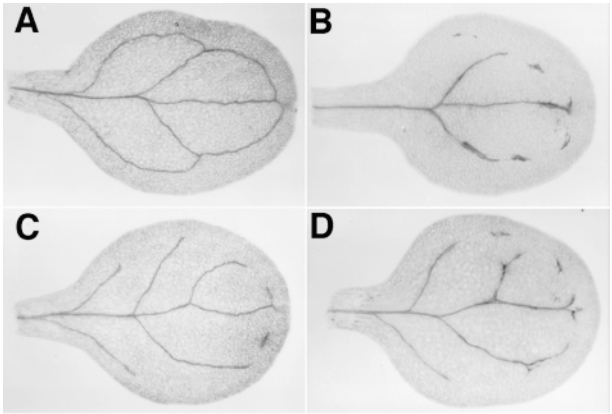

Figure 1. Vascular Bundle Patterns in Cleared Cotyledons.

(A) Wild type.
(B) *cvp1.*
(C) *cvp2.*
(D) *cvp1 cvp2.*
Magnification ×15.

eny from 29 of these M_2 plants displayed mutant cotyledon xylem patterns, although many of these plants produced a mixture of mutant and wild-type phenotypes. Plants from most of the putative mutant lines also displayed other developmental defects, including sterility, misshapen leaves, loss of apical dominance, and markedly delayed flowering times.

Two putative mutant lines were initially chosen for further study based on three criteria: (1) each showed expression of the mutant phenotype in all M_3 seedlings (Figures 1B and 1C); (2) the gross morphology and growth rate of the adult plants appeared normal (discussed below); and (3) the mutant phenotypes segregated as single recessive nuclear mutations in genetic crosses, as shown in Table 1. The genes identified by these mutations were named *CVP1* and *CVP2.* F_1 seedlings produced from genetic crosses between *cvp1* and *cvp2* mutant strains displayed wild-type vascular patterns, indicating that *CVP1* and *CVP2* represent different complementation groups (Table 1). Four different recessive mutant alleles of *cvp1* and three different recessive mutant alleles of *cvp2* have been identified and confirmed by complementation tests (see Methods). The different mutant alleles of *CVP1* and *CVP2* share characteristic phenotypes, although they differ in severity. We conducted all experiments described here with the first alleles identified for each gene.

Table 1. Genetic Segregation of the Phenotypes of the *cvp1* and *cvp2* Mutants

Cross[a]	Generation	Cotyledon Phenotype	
		Wild Type	Mutant
cvp1 × *CVP1*	F_1	24	0
	F_2	225	68[b]
cvp2 × *CVP2*	F_1	24	0
	F_2	179	52[c]
cvp1 × *cvp2*	F_1	12	0
cvp1 cvp2 × *cvp1*	F_1	0	16[d]
cvp1 cvp2 × *cvp2*	F_1	0	17[e]

[a] All genotypes represent homozygous loci.
[b] $\chi^2 = 0.3$.
[c] $\chi^2 = 0.5$.
[d] All cotyledons displayed the phenotype of the *cvp1* mutant.
[e] All cotyledons displayed the phenotype of the *cvp2* mutant.

Cotyledon Vascular Phenotypes of *cvp1* and *cvp2* Mutants

The xylem strand patterns in *cvp1* mutant cotyledons appeared to be discontinuous, although the exact pattern varied between individuals (Figure 1B). Some xylem strands appeared thicker than those in wild-type cotyledons, and examination under higher magnification revealed that these regions were characterized by unusually large numbers of xylem tracheary cells (Figures 1B and 2D). Isolated patches of multiple tracheids, apparently unconnected to other xylem strands, also were commonly observed.

In *cvp2* fully expanded cotyledons, all xylem strands appeared to be of normal thickness but contained additional lateral veins compared with wild-type cotyledons, and most (214 of 288) were characterized by the absence of closed distal loops (Figure 1C), which was not observed in wild-type cotyledons. *cvp2* cotyledons that displayed two closed loops also showed additional branches of vascular bundles and were clearly distinguished from wild-type cotyledons (74 of 288). Additional "spurs" of xylem were also more prevalent in *cvp2* cotyledons than in the wild type, resulting in a more highly reticulated pattern. Short stretches of isolated, apparently unconnected xylem strands were observed, although less frequently than in *cvp1* mutants. The unconnected xylem strands in *cvp1* and *cvp2* mutants were not observed in cotyledons from wild-type plants.

To determine whether the observed pattern of xylem strands coincided with the spatial pattern of phloem tissue, we stained cotyledons with aniline blue to visualize callose, which accumulates in phloem sieve cells (see Methods). As shown in Figure 2, fluorescence microscopy indicated that fluorescent strands, representing phloem tissue (Figures 2A, 2C, and 2E), showed a distribution similar to xylem strands (Figures 2B, 2D, and 2F) in both wild-type and *cvp* cotyledons. This result suggests that the effects of *cvp1* and *cvp2* mutations are not specific to xylem tissue, but appear to affect the vascular bundles as a whole, and therefore may act at an early step in vascular differentiation.

In general, however, *cvp1* and *cvp2* seedlings appeared very similar in overall size and morphology to wild-type seedlings (Figure 3). The cotyledons (Figures 3A to 3C) and root growth (Figures 3E to 3G) were indistinguishable from the wild type. Moreover, cleared roots of *cvp1* showed that the central vascular cylinder contained uniformly aligned vascular cells similar to wild-type roots (Figures 3I and 3J). Root cell anatomy also was examined in transverse sections, revealing that *cvp1* and wild-type cells were arranged similarly and were of similar size and shape (Figures 3K and 3L). Based on wild-type appearance of the *cvp* mutants, aberrant vascular patterning does not appear to compromise photosynthetic competency.

A *cvp1 cvp2* double mutant strain was identified by scoring the cotyledon vascular patterns of F_2 seedlings segregating for both *cvp1* and *cvp2* mutations. To confirm the identity of the double mutant strain, we performed test crosses to single mutant tester strains, and the vascular patterns in cotyledons from F_1 seedlings were scored to determine genetic complementation (Table 1). The phenotype of the double mutant appeared additive, in that the xylem strands contained additional cells but were more highly branched (Figure 1D), but nevertheless showed a seedling morphology indistinguishable from that of the wild type (Figures 3D and 3H). The cotyledon phenotypes of *cvp1* and the *cvp1 cvp2* double mutants often were difficult to distinguish,

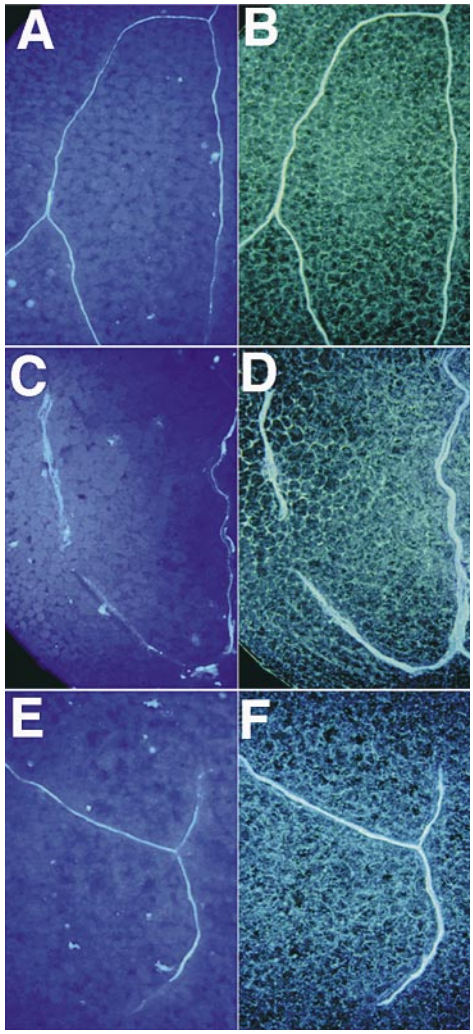

Figure 2. Correlation of Phloem Patterns with Xylem Patterns.

(A), **(C)**, and **(E)** Fluorescence microscopy of phloem sieve cells stained with aniline blue.

(B), **(D)**, and **(F)** Corresponding dark-field images of xylem elements. Wild-type cells are shown in **(A)** and **(B)**, *cvp1* cells are shown in **(C)** and **(D)**, and *cvp2* cells are shown in **(E)** and **(F)**. Magnification ×30.

however, which, in conjunction with the unknown molecular nature of the alleles, made the epistatic relationship between *cvp1* and *cvp2* unclear.

The *cvp1* and *cvp2* mutants were backcrossed to the wild-type Columbia strain and then crossed to the polymorphic Landsberg *erecta* strain. DNA from mutant F_2 segregants was prepared and used to identify linked polymorphic markers (see Methods). Figure 4 shows that *CVP1* and *CVP2* both map to chromosome 1, at approximate positions 19 and 9 centimorgans, respectively. Break point analysis revealed that *cvp1* is centromeric, and *cvp2* telomeric, to the *NCC1* molecular marker (Konieczny and Ausubel, 1993). *CVP1* is positioned on chromosome 1 in close proximity to *MONOPTEROS* (*MP*), a gene required for establishment of the basal region of Arabidopsis seedlings (Mayer et al., 1991). Seedling–lethal mutant alleles of *MP* that disrupt the entire root system have been described (Berleth and Jürgens, 1993). In the cotyledons of weaker *mp* alleles, disrupted vascular bundles similar to those seen in *cvp1* cotyledons also have been observed (Przemeck et al., 1996). Although the root in *cvp1* is unaffected by the mutation (Figures 3F, 3J, and 3L), given the apparent similarity of vascular patterns in *cvp1* and *mp* mutants and their tight genetic linkage, it is possible that *CVP1* and *MP* are the same gene. However, a complementation test performed between *mp* and *cvp1* mutant alleles revealed that the two genes are not allelic (see Methods). In addition, sequence analysis of genomic DNA isolated from *cvp1* mutant plants showed no sequence variations from the published wild-type *MP* sequence (data not shown). No other vascular patterning mutants with similar phenotypes that map in the same chromosomal position have been reported.

cvp Mutations Affect Establishment of Procambial Tissue in Cotyledons

At least two different models of *CVP1* and *CVP2* action can be postulated: either (1) mutations in *cvp1* and *cvp2* primarily affect the patterning of procambial tissues (the precursors to mature vascular cells) in cotyledons, which then differentiate normally, or (2) these mutations affect only the final differentiation of otherwise normally patterned procambial tissue. If the first model is correct, then the pattern of procambial tissues in *cvp1* and *cvp2* mutant cotyledons ought to appear disrupted during the developmental stage at which the pattern is first evident.

To distinguish between these two models, we dissected developing embryos from wild-type and mutant seed pods (siliques) ~140 hr after fertilization and observed them in whole-mount preparations, as shown in Figure 5. At this stage in development, the procambial tissues have not begun differentiating into xylem and phloem, an event that initiates 36 hr after germination (Dharmawardhana et al., 1992). Procambial tissue could be observed in wild-type embryonic cotyledons and was arranged in a pattern identical to that of differentiated vascular bundles in mature cotyledons (Figure 5A). This result indicated that the primary vascular pattern in cotyledons is established during embryogenesis and precedes final differentiation of xylem and phloem cell types. In *cvp1* embryos, the pattern of procambial tissue differed from that of the wild type. This tissue displayed patterns consistent with those of differentiated vascular bundles in mature *cvp1* cotyledons (Figure 5B). Patterning defects, specifically branched unclosed loops of procambium, also were observed in most *cvp2* embryos, although these defects were often more subtle and less easily scored than the

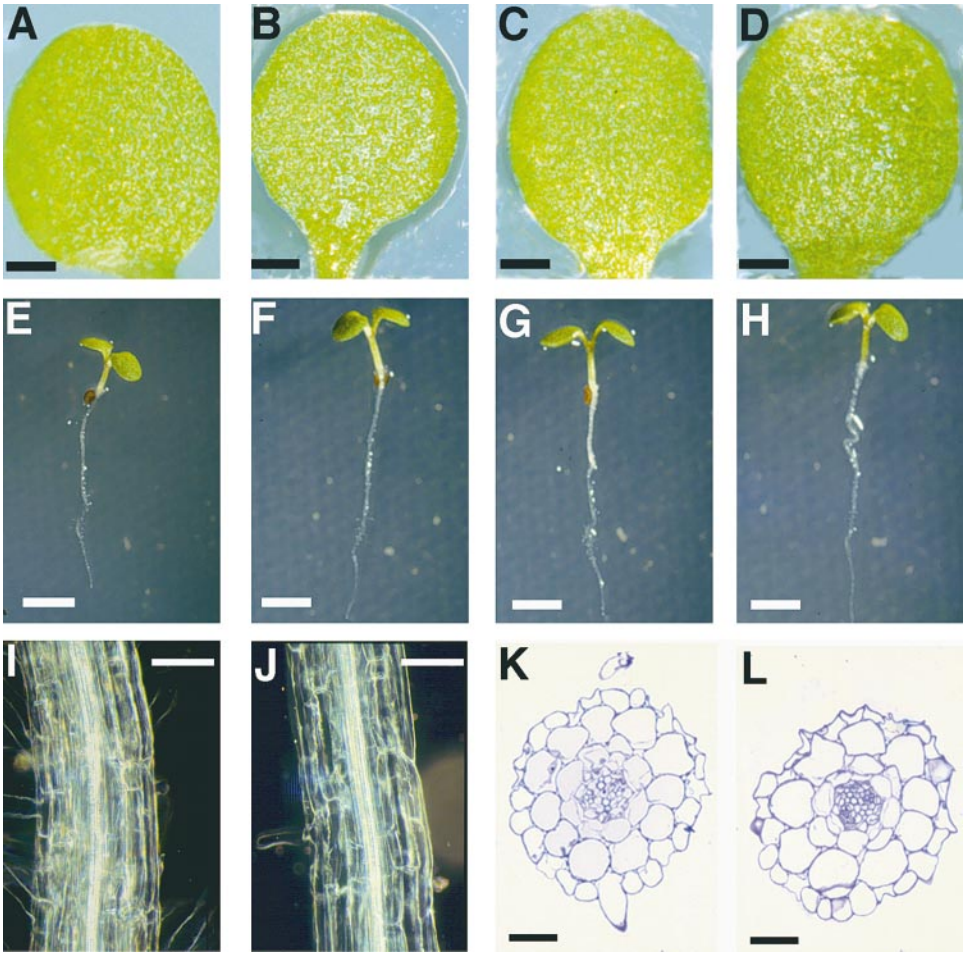

Figure 3. Wild-Type Morphology and Root Anatomy of *cvp* Mutants.

(A) to **(D)** Detached cotyledons from 7-day-old seedlings show wild-type morphology in the wild type **(A)** and in the *cvp1* **(B)**, *cvp2* **(C)**, and *cvp1 cvp2* **(D)** mutants.
(E) to **(H)** Seven-day-old seedlings show wild-type seedling growth and phenotype. **(E)** shows a wild-type seeding, **(F)** shows a *cvp1* seedling, **(G)** shows a *cvp2* seedling, and **(H)** shows a *cvp1 cvp2* seedling.
(I) and **(J)** Longitudinal view of 7-day-old cleared roots of the wild type **(I)** and *cvp1* **(J)**. **(J)** shows axialization in the vascular cylinder of *cvp1.*
(K) and **(L)** Transverse sections of wild type **(K)** and *cvp1* **(L)**. In **(L)**, 7-day-old roots illustrate wild-type internal anatomy of *cvp1.*
Bars in **(A)** to **(D)** = 250 μm; bars in **(E)** to **(H)** = 500 μm; bars in **(I)** and **(J)** = 80 μm; bars in **(K)** and **(L)** = 25 μm.

alterations in *cvp1* embryos (Figure 5C). The patterns observed in *cvp1 cvp2* double mutant embryos were similar to those of *cvp1* embryos (Figure 5D). Taken together, these data indicate that *cvp1* and *cvp2* directly affect the patterning of procambial tissue in cotyledons.

cvp Cotyledon Anatomy

Histological characterization of *cvp* cotyledons was performed by examination of serial sections of resin-embedded seedlings in both paradermal (i.e., parallel to the cotyledon surface) and transverse orientation, as shown in Figure 6. In 5-day-old cotyledons, most vascular cells are in immature stages. In wild-type cotyledons, cells committed to a vascular fate divide longitudinally (long axis parallel to the axis of the provascular strand) to conform to the directional orientation of the provascular strand (Figure 6A). When vascular cells mature, these interconnected cells will provide a conduit for transport of nutrients. Paradermal sections of *cvp1* cotyledons revealed a highly disorganized vascular system. In *cvp1*, the midvein in all cases was found to be similar to a wild-type midvein (Figure 6B), with the exception of the most apical end. However, the provascular cells of lateral

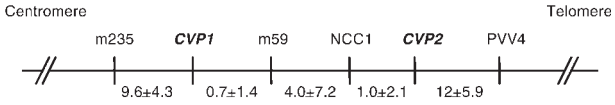

Figure 4. Map Positions of *CVP1* and *CVP2.*

Numbers represent recombination frequencies ±SE between *CVP* genes and linked molecular markers. The recombination frequencies of m235, *CVP1*, and m59 were determined from scoring 72 F_2 plants (144 chromosomes), and the frequencies of NCC1, *CVP2*, and PVV4 were determined from scoring 43 F_2 plants (86 chromosomes).

veins divide in abnormal planes, in effect establishing alternate directions of growth to the provascular strand (Figure 6C). The cells did not elongate normally and were improperly aligned, thus failing to establish longitudinal files of cells (Figures 6C and 6D). In addition, there were abnormally large, often misshapen cells positioned in aberrant planes within the vascular bundle (Figure 6D). Although some of these large cells showed characteristics of maturing vascular cells, such as thickened cell walls and the presence of annular rings (tracheary elements only), other large cells lacked all vascular qualities and appeared to be parenchyma cells that are inappropriately positioned within a vascular bundle.

Paradermal sections of *cvp2* vascular bundles revealed no histological differences when compared with the wild type. Vascular cells of *cvp2* cotyledons elongated appropriately and formed longitudinal files (Figure 6E). As predicted from the cleared cotyledon analysis, paradermal sections of *cvp1 cvp2* double mutants exhibited characteristics of both mutants (Figure 6F). Isolated veins were observed in *cvp1* and *cvp1 cvp2* cotyledons (Figure 6F), representing the isolated tracheids that were observed in cleared sections. There were no indications that these isolated veins join a nearby vein, suggesting a discontinuous origin. These results further support our observation that the *cvp* are defective in the establishment of the vascular pattern at the procambial stage and not in the differentiation of vascular cells, because all stages of vascular differentiation are observed.

Figure 7 displays transverse sections through the lamina of wild-type (Figure 7A) and mutant cotyledons (Figures 7B to 7E) which indicate that the *cvp1* and *cvp2* mutations do not affect the internal anatomy of the cotyledon (Figures 7A to 7E). In 9-day-old cotyledons, mature xylem and phloem cells were observed within *cvp* mutant vascular bundles in the appropriate collateral arrangement, with xylem on the dorsal side and phloem on the ventral side (data not shown). One characteristic of *cvp2* mutants is a failure to form closed loops (Figure 1C) such that lateral veins terminate freely within the spongy mesophyll, possibly resulting from a loss of guidance from the veins to which they normally would form a junction. In wild-type Arabidopsis, this event is restricted to veinlets, which terminate freely within an areole rather than connecting to an existing vein. This presumably is due to a loss of competence of the provascular strand to form a vein, although definitive proof has not been presented (Nelson and Dengler, 1997). Transverse serial sectioning was performed on early terminating veins in *cvp2* mutants in an attempt to associate a histological defect with the vein endings. Wild-type veins usually diminish in girth progressively from their point of origin. It is apparent that *cvp2* lateral veins became progressively less seriated (fewer vascular elements) because fewer cells are recruited to a vascular fate (from 10 vascular cells to one vascular cell, as shown in Figures 7D and 7E, respectively). However, there was no discernible cellular abnormality in the surrounding mesophyll cells (Figures 7D and 7E). These data suggest that the *cvp1* and *cvp2* mutations specifically affect the pattern of differentiated vascular tissues in cotyledons without disrupting leaf anatomy.

Phenotypes of Additional Organs in *cvp* Mutants

In general, the growth and morphology of *cvp* mutant plants were markedly similar to those of wild-type plants. Flowering time and the number of leaves produced before flowering were unaffected in the mutants, and the structure of *cvp* flowers displayed no obvious morphological differences and no reduction in fertility compared with wild-type flowers (data not shown). Similarly, there were no obvious differences between the growth rates (Figures 3E to 3H), cellular morphologies (data not shown), or organization of roots of the *cvp* mutants and wild-type plants (Figures 3E to 3L).

To determine whether the *cvp* mutations are cotyledon specific or act more generally, we compared the vascular

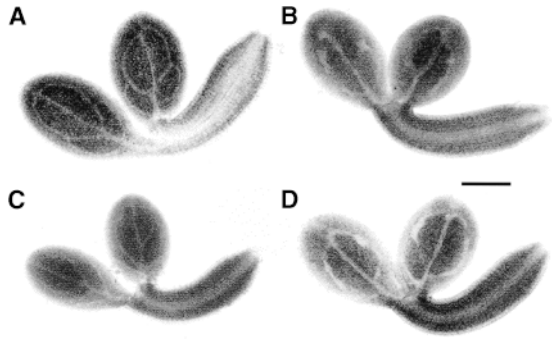

Figure 5. Procambium Patterns in Embryonic Cotyledons.

Procambial tissue is observed as strands of lightly stained cells in the embryonic cotyledons.
(A) Wild type.
(B) *cvp1.*
(C) *cvp2.*
(D) *cvp1 cvp2.*
Bar in **(D)** = 31 μm for **(A)** to **(D)**.

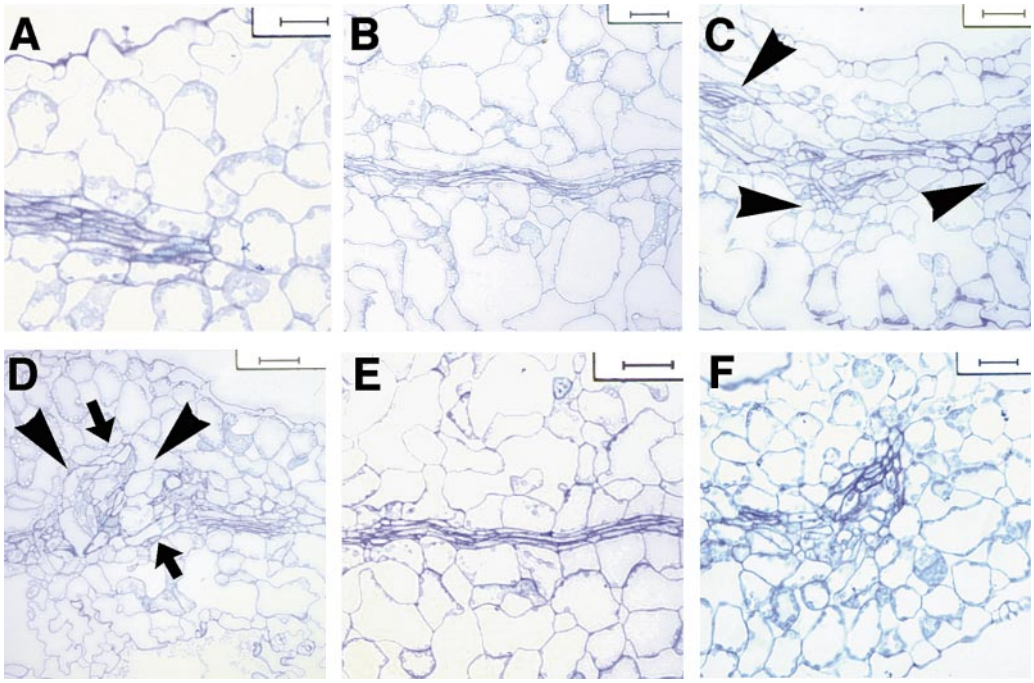

Figure 6. Anatomy of Cotyledon Vascular Bundles in *cvp* Mutants Visualized by Paradermal Plastic Sectioning of 5-Day-Old Cotyledons.

(A) Wild-type vein shows longitudinal files of elongating provascular cells. Vascular bundles normally are oriented obliquely, resulting in sections with short stretches of veins.
(B) *cvp1* wild-type-like vein.
(C) *cvp1* mutant vein illustrates improper alignment of cell files and incorrect division planes of provascular cells (arrowheads).
(D) Abnormal cell expansion within *cvp1* vascular bundle (arrowheads). Arrows indicate misshapen xylem cells (tracheary elements) that stain a turquoise blue with toluidine blue dye.
(E) *cvp2-1* vein showing elongated provascular cells arrayed in longitudinal files.
(F) *cvp1 cvp2* mutant vein that is isolated (discontinuous) from other veins.
Bar in **(A)** = 31 μm; bars in **(B)** to **(E)** = 40 μm; bar in **(F)** = 25 μm.

bundle patterns in the first true leaves of wild-type and *cvp* seedlings in whole-mount preparations (see Methods). Unlike the cotyledon venation pattern, the vascular pattern in *cvp1* mutant leaves did not show any discontinuity or histological defects and was indistinguishable from that of the wild type, as shown in Figures 8A and 8B. *cvp2* and *cvp1 cvp2* leaves (168 of 190) displayed unconnected xylem strands similar to those seen in *cvp2* mutant cotyledons (Figures 8C and 8D). Specifically, as deduced from a quantitative comparison between cleared wild-type and *cvp2* leaves, 47% (475 of 1010) of *cvp2* tertiary veins failed to connect to secondary (lateral) veins, and 97% (116 of 120) of *cvp2* quaternary veins appeared as isolated veins (Figures 8C and 8D). In wild-type leaves, intramarginal veins branch from secondary veins to generate extensions typically in the form of small closed loops (~80% of loops are closed; 356 of 440) along the margins of the leaf (Figure 8A). A *cvp2* leaf at the same stage has ~50% fewer intramarginal veins, which rarely connect to form a closed loop (Figure 8C; 30 of 208). In *cvp2* and *cvp1 cvp2* leaves, there are fewer tertiary and quaternary veins, resulting in less reticulation compared with wild-type leaves (Figures 8C and 8D). Consistent with our observations of mutant cotyledon morphology, the size and shape of leaves from *cvp1* and *cvp2* single mutant strains, as well as the double mutant strain, were indistinguishable from those of wild-type plants (Figures 8A to 8D). *cvp2* cauline leaves (Figures 8E to 8H) and sepals (data not shown) also showed an increase in the number of free vein endings when compared with the wild type. These results indicate that the *cvp2* mutation affects both embryonic and adult development.

An increase in the number of free vein endings may indicate a delay in vein initiation in *cvp2* leaves. Studies of the embryonic patterns suggested that there was no delay in *cvp2* vein initiation, because the procambial cell pattern, which establishes the final venation pattern, did not appear to be delayed when compared with the wild type (Figure 5). In addition, a consequence of delayed vein initiation in *cvp2*

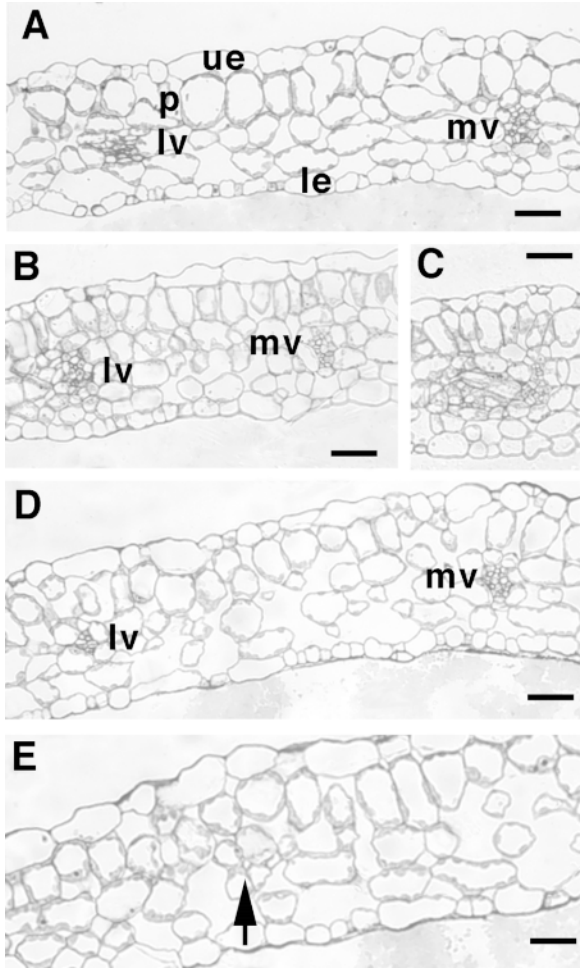

Figure 7. Transverse Sections of Cotyledons from 5-Day-Old Seedlings.

(A) Wild type.
(B) *cvp1* showing normal midvein and abnormal lateral vein.
(C) *cvp1* showing misaligned lateral vein in longitudinal orientation.
(D) *cvp2* showing midvein and a lateral vein composed of 10 vascular elements.
(E) *cvp2* with arrow designating same lateral vein as shown in **(D)** at a distal point and composed of a single vascular element.
Note the wild-type epidermal and mesophyll cells (particularly the palisade cells) in **(B)** to **(E)**. le, lower epidermis; lv, lateral vein; mv, midvein; p, palisade cells (which elongate and are arranged parallel to each other within the adaxial subepidermal layer); ue, upper epidermis.
Bars in **(A)** to **(D)** = 31 μm; bar in **(E)** = 25 μm.

leaves would be fewer vascular elements. This phenotype would have been apparent in whole-mount preparations but was not observed (Figures 1C, 1D, and 8). To investigate further the timing of *cvp2* vein initiation, we conducted a detailed analysis by using the more amenable rosette leaf. A developmental stage analysis of wild-type and *cvp2* first rosette leaves was performed by monitoring tracheary element lignification to determine whether *cvp2* veins were initiated as they are in the wild type. Our observations of wild-type venation patterns in rosette leaves are in agreement with those of others (Telfer and Poethig, 1994; Kinsman and Pyke, 1998; Candela et al., 1999). At 7 days after sowing, lignification of the midvein had been initiated in both wild-type and *cvp2* leaves (Figures 8I and 8J). At 9 days, the apical loops differentiated into xylem in both wild-type and *cvp2* leaves; however, one open apical loop was observed in a *cvp2* leaf (Figures 8K and 8L). At 12 days, the first rosette leaf was fully expanded and the venation pattern was complete, with all secondary, tertiary, and quaternary veins present in the wild type and mutant (Figures 8M and 8N). However, as described previously, *cvp2* tertiary and quaternary veins displayed an increase in unconnected vein endings. At a later time point (16 days after sowing), an increase in free vein endings remained a feature of *cvp2* leaves (Figures 8O and 8P). These studies suggest that the defect in *cvp2* venation pattern is due to premature termination of veins and not due to a delay in vein initiation.

A subtle but surprising phenotype was observed in the inflorescence stems of *cvp1* mutants. The internode distance between siliques appeared less regular in *cvp1* strains than in the wild type, and it was highly compact in ~10% of *cvp1* inflorescence stems (7 of 68), as shown in Figure 9C. This shortened internode phenotype usually was observed at the apex of primary and secondary inflorescence stems and was not observed in *cvp2* mutant strains. Histological analysis of stem sections from affected regions of inflorescence stems from *cvp1* and *cvp1 cvp2* double mutant plants showed an increased amount of vascular tissue, most notably xylem and lignified sclerenchyma, in the inflorescence stem (Figure 9B). The apparent overproduction of vascular tissue was observed only in regions displaying reduced internode distances, whereas the amount and organization of vascular tissue in unaffected regions were similar to those observed in wild-type stems (Figure 9A). These observations indicate that the internode spacing defects in *cvp1* mutants correlate to alterations in vascular tissue differentiation. Interestingly, *cvp1 cvp2* double mutant strains displayed a higher proportion of inflorescence stems bearing this compact internode phenotype (17 of 51), indicating that *cvp2* mutations can enhance this phenotype in *cvp1* genetic backgrounds.

Auxin Biosynthesis, Perception, and Transport Do Not Appear to Be Affected in the *cvp* Mutants

Auxin has been shown to play a critical role in vascular differentiation, in particular as a result of polar auxin transport through plant tissues. To examine whether levels of free IAA were affected in the *cvp* mutants, we measured free IAA in 9-day-old seedlings by the highly sensitive gas chromatography–selected ion monitoring–mass spectrometry method

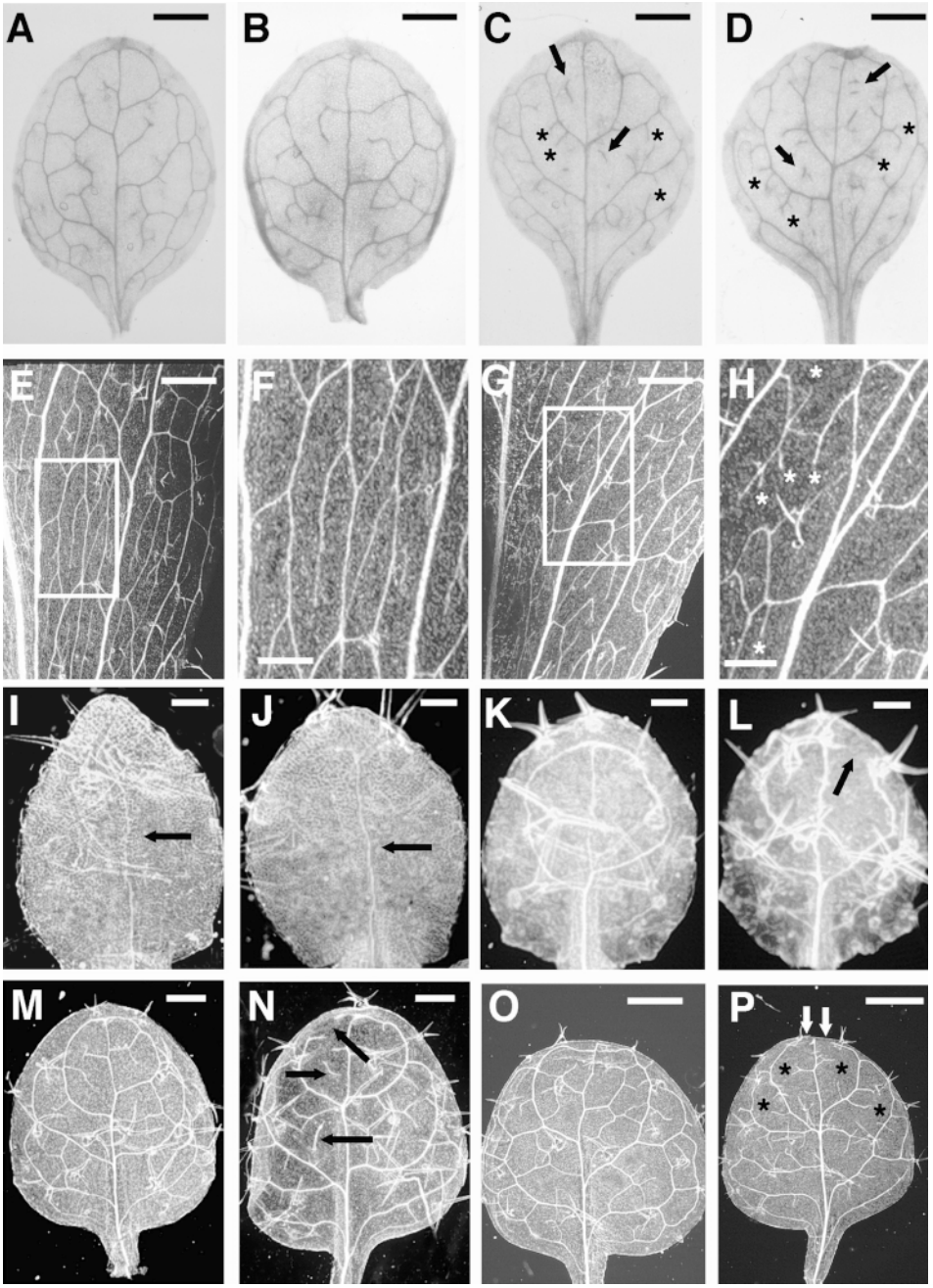

Figure 8. Vascular Bundle Patterns in *cvp* Leaves.

(A) to **(D)** Safranin-*O*–stained first rosette leaves from 14-day-old wild-type **(A)**, *cvp1* **(B)**, *cvp2* **(C)**, and *cvp1 cvp2* **(D)** plants. In **(B)** and **(D)**, note the wild-type venation pattern in *cvp1* and unattached vascular bundles (arrows) and premature termination of tertiary veins (only a few are indicated with asterisks) in the *cvp2* and *cvp1 cvp2* leaves.

(E) to **(H)** Cleared cauline leaves from wild-type (**[E]** and **[F]**) and *cvp2* (**[G]** and **[H]**) plants show the increase in free vein endings (indicated with asterisks in **[H]**) in *cvp2* mutants. Boxed regions in **(E)** and **(G)** are shown at a higher magnification in **(F)** and **(H)**, respectively.

(I) to **(P)** Developmental stage analysis of the first rosette leaf of the wild type (**[I]**, **[K]**, **[M]**, and **[O]**) and *cvp2* (**[J]**, **[L]**, **[N]**, and **[P]**) at 7 days (**[I]** and **[J]**), 9 days (**[K]** and **[L]**), 12 days (**[M]** and **[N]**), and 16 days (**[O]** and **[P]**) after sowing shows that there is no delay in vein initiation in *cvp2* mutants. Arrows indicate the midvein (**[I]** and **[J]**), an open apical loop in a *cvp2* mutant leaf **(L)**, unconnected *cvp2* veins **(N)**, and open apical loops **(P)**. Asterisks indicate some of the free tertiary vein endings **(P)**. Transparent spiked structures are trichomes.

Bars in **(A)** to **(D)**, **(E)**, **(G)**, **(O)**, and **(P)** = 800 μm; bars in **(F)** and **(H)** = 300 μm; bars in **(I)** and **(J)** = 80 μm; bars in **(K)** and **(L)** = 250 μm; bars in **(M)** and **(N)** = 320 μm.

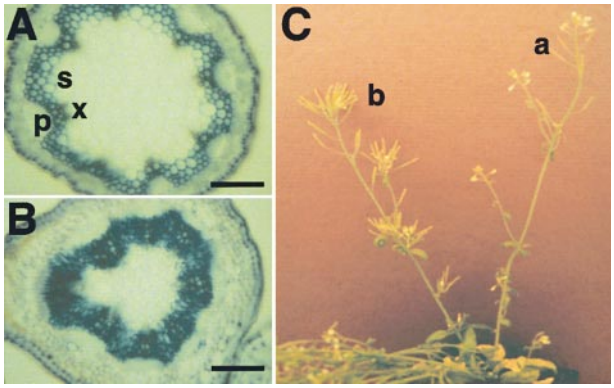

Figure 9. Inflorescence Stems in *cvp1* Plants.

(A) Transverse section of inflorescence stem displaying wild-type internode lengths. Xylem (x) and lignified sclerenchyma (s) cell walls appear dark blue. Lightly staining phloem bundles (p) are associated with xylem.

(B) Transverse section of inflorescence stem displaying decreased internode lengths. Note increased production of xylem and lignified sclerenchyma.

(C) *cvp1* plant displaying inflorescence stems with normal (a) and decreased (b) internode lengths.

Bars in **(A)** and **(B)** = 400 μm.

(Chen et al., 1988). As shown in Table 2, there are no statistically significant deviations in free IAA levels between wild-type and *cvp* seedlings, suggesting that the *cvp* mutations do not affect auxin biosynthesis. To determine whether the *cvp* mutations cause alterations in sensitivity or resistance to auxin, we germinated seeds for 10 days on medium containing different concentrations of IAA or 2,4-D (a synthetic auxin). The data in Figures 10A and 10B indicate that the *cvp* single and double mutant strains showed levels of root growth inhibition identical to those in the wild-type strain. Similarly, the *cvp* mutant strains showed neither altered sensitivity nor resistance to triiodobenzoic acid, a compound known to inhibit polar auxin transport (Okada et al., 1991; Figure 10; see Methods). Similar results were found for two additional inhibitors of polar auxin transport, 9-hydroxyfluorene-9-carboxylic acid and *trans*-cinnamic acid (data not shown).

To assay directly for basipetal auxin transport in inflorescence stems of wild-type and *cvp* plants, we monitored the transport of ^{14}C-labeled IAA through excised stem segments. Data in Figure 11 show that basipetal auxin transport is virtually identical in wild-type and mutant stems, indicating that polar auxin transport is not generally affected in the *cvp* mutants. These results, in addition to the overall wild-type appearance of *cvp1* and *cvp2* mutant plants, suggest that the *cvp* mutations do not cause gross alterations in auxin biosynthesis, perception, or polar auxin transport, although it remains possible that free IAA levels and rates of auxin transport are affected specifically in cotyledon vascular tissues in the *cvp* mutant strains.

DISCUSSION

The phenotypes of the *cvp1* and *cvp2* mutants suggest that aberrant vascular patterning is the primary defect in these plants. The general morphology and differentiation of epidermal and mesophyll cells in *cvp1* and *cvp2* mutant cotyledons appear identical to the wild type, despite the substantial alteration of vascular bundle patterns observed. Furthermore, vascular cell differentiation appears unaffected in the mutant veins, because all stages of differentiation are represented. It is not known whether water and nutrient transport are affected in *cvp* cotyledons or leaves, although the wild-type growth rate of these strains suggests that any effects must be relatively minor. The analysis of developing embryos indicates that *cvp1* and *cvp2* mutations disrupt the spatial arrangement of the procambium in developing cotyledons and therefore that the *cvp* mutations act at one of the earliest observable stages of vascular development. *cvp1* mutants demonstrate a failure to promote cell axialization as characterized by misguided provascular strand formation, reduced cell elongation, and expanded, misshapen vascular cells. No such observable defect is detectable in *cvp2* mutants. In addition to their effects on cotyledon vascular bundles, mutations in *cvp1* and *cvp2* cause alterations in the vasculature of vegetative leaves and/or inflorescence stems. It will be interesting to determine whether *CVP1* and *CVP2* disrupt procambium patterning in nonembryonic tissues in a manner similar to that observed in developing cotyledons. To follow this process, we have crossed various reporter

Table 2. Quantitation of Free IAA in Wild-Type and *cvp* Seedlings

Genotype	Free IAA ±SD[a]	*t* Value[b]
Wild type	0.033 ± 0.032	ND[c]
cvp1-1	0.029[d]	ND
cvp2-1	0.034 ± 0.015	0.1037
cvp1-1 cvp2-1	0.023 ± 0.009	0.9915

[a] Free IAA values are given as the mean ±SD in micrograms per gram fresh weight of tissue. Samples were assayed in the triplicate unless otherwise noted.

[b] Student's *t* test was applied for statistical analysis. *t* values were determined between the free IAA level of the mutant and wild type. A *t* value of ⩾2.776 would indicate a significant difference with a 95% confidence interval.

[c] ND, not determined.

[d] Assayed in duplicate.

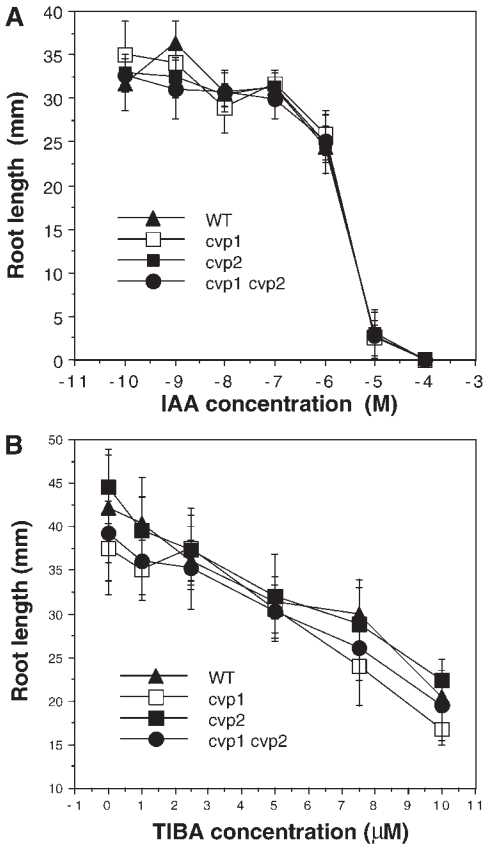

Figure 10. Sensitivity to Auxin and an Inhibitor of Polar Auxin Transport.

Plants were grown on synthetic media containing different concentrations of either IAA **(A)** or triiodobenzoic acid (TIBA) **(B)**, an inhibitor of polar auxin transport. Root lengths were measured after growth on these media for 10 days. WT, wild type.

genes expressed specifically in Arabidopsis procambial cells (F.M. Carland, N. Kho, and T. Nelson, unpublished data) into *cvp1* and *cvp2* mutant strains as molecular markers for procambium.

CVP1 and *CVP2* may be involved in generating and/or perceiving positional signals that specify the spatial arrangement of procambium in developing tissues. *cvp1* mutants have many similarities to *mp* mutants, with the exception that root development is unaffected. The recent molecular isolation of *MP* revealed that the gene is a member of the auxin response factor (*ARF*) gene family, which are transcription factors that have been shown to bind to functional auxin-responsive promoter elements of the *AUX/IAA* gene family (Kim et al., 1997; Ulmasov et al., 1997; Hardtke and Berleth, 1998). These results provide convincing molecular evidence of a role for auxin in mediating vascular pattern formation. The diversity of the *ARF* and *AUX/IAA* gene families and the potential for homodimerization and heterodimerization among its members suggest that multiple roles of auxin in plant development rely on temporally and spatially regulated subsets of these complexes that mediate differential expression of downstream auxin-inducible genes (Kim et al., 1997). This hypothesis is supported by the recent findings that mutations in other members of the *ARF* gene family, including *ETTIN/ARF3*, affect different developmental pathways (Sessions et al., 1998). The *ettin* mutations specifically affect floral organ number and gynoecial apical–basal patterning (Sessions et al., 1998). Given the similarity in *mp* and *cvp1* venation pattern defects, it is possible that *CVP1* is a member of the *ARF* or *AUX/IAA* gene family, and activates downstream target genes specifically involved in shoot vascular cell axialization and not in root development.

cvp2 mutants are characterized by a failure of vascular bundles to form closed loops in the cotyledons and in foliar leaves. This observation suggests that there is an apparent loss of developing provascular strand guidance, possibly due to signaling defects, causing premature vein termination, and posits a role for *CVP2* in promoting the progression of provascular strand formation. Based on the hypothesis (see below) that the polarized flow of auxin in a source–sink manner is required to establish the venation pattern, *CVP2* may be involved in the transduction or perception of auxin-mediated signals. Alternatively, *CVP2* may

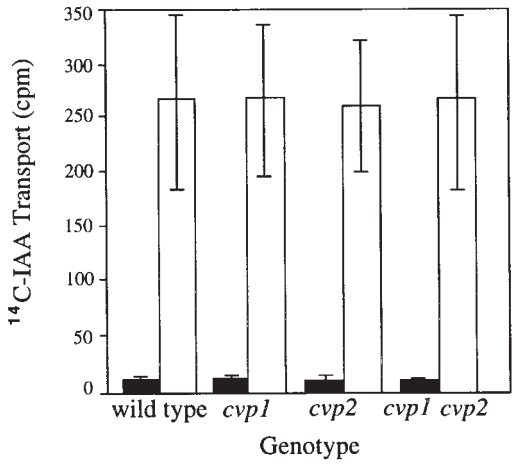

Figure 11. Transport of ^{14}C-IAA in Excised Inflorescence Stems of the Wild Type and *cvp* Mutants.

Data represent the average counts per minute of ^{14}C-IAA contained in a 0.5-cm excised segment from detached stems after incubation in medium and were calculated from ~100 samples of each genotype from four separate experiments. Error bars indicate ±SD. Filled bars indicate acropetal transport; open bars indicate basipetal transport.

be involved in an auxin-independent process. Elucidation of the molecular mechanisms by which *CVP2* acts, however, awaits identification of its gene product.

A large body of evidence indicates that auxin transport plays an important role in the differentiation of vascular tissues in plants (Aloni, 1987; Sachs, 1991b). Through a series of elegant surgical experiments, Sachs has demonstrated that exogenously administered auxin can induce existing parenchyma cells to redifferentiate into new vascular bundles in wounded bean and pea stems (Sachs, 1991a). Source–sink relationships are proposed to determine the position of these new vascular strands, so that files of parenchyma cells that transport auxin most efficiently from its source toward a sink, such as another vascular bundle or root, are induced to differentiate into vascular tissues. As files of cells begin differentiating into vasculature, their ability to transport auxin from surrounding cells increases, creating a positive feedback. These experiments have led to the "canalization" model, which proposes that the final pattern of vascular bundles reflects the preferred paths of polar auxin transport through files of cells, which is considered to be stochastic and not determined by any genetically controlled "prepattern" (Sachs, 1991a, 1991b). This model is consistent with two important observations: (1) auxin is transported preferentially through vascular bundles (Rubery, 1987); and (2) the position of newly differentiated vascular bundles depends primarily on the position of the exogenous auxin source in these experiments (Sachs, 1991a).

The canalization model accounts well for the differentiation of existing parenchyma cells into xylem and phloem in mature tissues but is less suitable in explaining procambial patterning during early development. It is intriguing that the expression pattern of *MP* parallels the postulated flow of auxin described in the canalization theory and may reflect the role of *MP* in mediating downstream auxin-inducible genes (Hardtke and Berleth, 1998). Results from our study indicate that the patterning of procambial tissue is at least partly under genetic regulation, and that disrupting procambial patterns through mutation can alter the distribution of differentiated vascular bundles in mature tissues with no effect on vascular cell differentiation. The *cvp* single and double mutant strains showed no alteration, when compared with the wild type, in auxin biosynthesis, perception, or transport, as measured by conventional assays. Moreover, *cvp* strains do not exhibit the pleiotropic effects on root elongation, apical dominance, gravitropism (F.M. Carland and T. Nelson, unpublished data), and fertility observed for Arabidopsis mutants defective in auxin perception and transport. However, we cannot rule out the possibility that localized alterations within the cotyledons may have been undetectable in our assays. To explore further the possible role of *CVP* genes in auxin metabolism, we are constructing multiple mutant Arabidopsis strains to determine whether mutations in *AXR1* and *AXR2* (Estelle and Somerville, 1987; Lincoln et al., 1990; Timpte et al., 1994) that disrupt auxin signaling or mutations in *TRP2* (Last et al., 1991) that overproduce auxin (Normanly et al., 1993) alter the expression of the phenotype of *cvp* mutants. Furthermore, the recent cloning of members of the auxin transport efflux carrier family may provide insight into auxin transport defects in the *cvp* mutants (Chen et al., 1998; Gälweiler et al., 1998; Luschnig et al., 1998; Müller et al., 1998).

The ability of *cvp2* mutant alleles to enhance the shortened internode phenotype observed in *cvp1* mutant plants suggests that the products of these two genes interact. In addition, this interaction offers a means to identify other genes that control vascular development by screening for enhancers and suppressors of this phenotype in either *cvp1* or *cvp2* genetic backgrounds. Because we have identified four different mutant alleles of *cvp1* and three different alleles of *cvp2*, it seems unlikely that we will identify many additional genes by using the screen described here. In addition, mutants that specifically affect foliar venation pattern without altering morphology have not been identified by using mutagenesis screens (Carland and McHale, 1996; Candela et al., 1999). By screening for new mutations using the inflorescence phenotype, we may be able to identify a genetic pathway that incorporates *CVP1* and *CVP2* and controls vascular development in Arabidopsis. The ability to control the extent or patterning of vasculature in plants through genetic manipulation has important implications for our understanding of plant development as well as for horticulture and commercial manipulation of wood and fiber content.

METHODS

Plant Materials

Seeds (*Arabidopsis thaliana* ecotype Columbia) were grown either on a minimal plant nutrient medium supplemented with sucrose (PNS containing 0.7% agar; Haughn and Somerville, 1986) or in soil (Metro-Mix 200; W.R. Grace Co., Marysville, OK) under constant white light ($\sim$300 μE m^{-2} sec^{-1}).

Isolation and Genetic Characterization of *cvp* Mutants

A visual screen for vascular pattern mutants was performed on ethyl methanesulfonate–mutagenized M_2 Arabidopsis (ecotype Columbia) seeds. Briefly, M_2 seeds are the progeny of self-fertilized plants grown from seeds imbibed in 0.3% ethyl methanesulfonate for 16 hr before planting (M_1 generation); this process allows recovery of homozygous recessive mutations in the M_2 progeny (Estelle and Somerville, 1986). M_2 seed (from 10 different flats sown with 5000 M_1 seeds each) were surface-sterilized in 30% Clorox and 0.01% Triton X-100 for 10 min, washed in sterile water, and germinated on PNS agar medium. After germination and growth for 7 days under continuous white light, one cotyledon from each seedling was excised, incubated in 95% ethanol to clear chlorophyll, and examined under a dissecting microscope. Putative vascular pattern mutants were transferred to soil to generate self-fertilized M_3 progeny, which were examined in the same way to confirm transmission of the mutant

phenotype. Mutant strains of interest were backcrossed twice as males to the wild-type Columbia strain.

Genetic crosses were conducted by hand-pollinating emasculated immature flowers. Complementation analyses were performed by reciprocally crossing *cvp1* and *cvp2* plants and examining the cotyledon vascular patterns in the resulting F_1 seedlings. Mutant alleles of each gene were considered to be different if they were isolated from independent M_2 seed pools.

A *cvp1 cvp2* homozygous double mutant strain was obtained by crossing the homozygous single mutants to each other and scoring vascular phenotypes of the F_2 generation (see text). The identity of the double mutant strain was confirmed by test crosses to homozygous *cvp1* and *cvp2* single mutant strains.

The complementation test between *mp* and *cvp1-1* was performed by crossing *cvp1-1* homozygotes to mp^{T370} (kindly provided by T. Berleth, University of Toronto) heterozygous plants in reciprocal crosses. Two hundred and forty F_1 plants from 24 independent crosses were scored and found to be wild type, indicating complementation between the two genes.

Histological Characterization

For whole-mount preparations, two techniques were used. For stained specimens, wild-type and mutant cotyledons and first true leaves were fixed for 1 hr in acetic acid:95% ethanol (1:3), cleared for 1 to 3 hr in 25% chloral hydrate, dehydrated for 1 hr in 95% ethanol, and stained briefly (1 to 2 min) in 1% safranin-*O* (Sigma) in 95% ethanol. Cotyledons then were partly destained in 95% ethanol, hydrated through an ethanol series to water, and mounted on slides in 50% glycerol and 0.01% Triton X-100. For cleared leaf material, the specimens were fixed as described above and cleared sequentially in 70% ethanol for 30 min, 100% ethanol overnight, and 10% NaOH for 1 hr at 42°C. Specimens were mounted on slides in 50% glycerol and visualized on a Zeiss Axiophot microscope (Oberkochen, Germany) under dark-field illumination.

For visualization of callose in phloem sieve tube elements, cotyledons were fixed for 1 hr in acetic acid:95% ethanol (1:3), treated in 2 M NaOH for 1 hr, neutralized briefly in 50 mM $NaPO_4$, pH 6.8, and stained overnight in 0.005% aniline blue (Fisher Scientific) in 50 mM $NaPO_4$, pH 6.8. Fluorescence under UV light was visualized with a Zeiss Axiophot microscope equipped with a broad-band filter to detect 4′,6-diamidino-2-phenylindole.

For histological analysis, cotyledons from wild-type and *cvp* plants were fixed in 4% glutaraldehyde (16 to 48 hr at 4°C), dehydrated through a graded ethanol series to 95% ethanol, and stained at room temperature for 16 hr in 0.1% eosin (in 95% ethanol) to assist with specimen visualization. Specimens then were dehydrated with 100% ethanol and embedded in Spurr's medium (EM Sciences, Ft. Washington, PA). Paradermal and transverse sections (1 μm) were cut on a Sorvall MT2-B ultramicrotome (Newtown, CT). Sections were stained briefly with filtered 1% toluidine blue. Because veins are oriented obliquely, only short stretches of veins are visible within each section. Through serial sections, the venation pattern of the cotyledons was reconstructed. In this manner, the position of mutant veins and the appearance of isolated veins were determined.

Inflorescence stems from wild-type and *cvp* strains were sectioned (50 μm) on a Lancer Series 1000 Vibratome (Energy Beam Sciences, Agawam, MA); fixed in 50% ethanol, 10% acetic acid, and 5% formaldehyde for 15 min; and cleared of chlorophyll in 95% ethanol for 15 min. Sections were rehydrated through an ethanol series into water, stained with 0.1% toluidine blue, and photographed on a Zeiss Axiophot microscope.

Isolation of Embryos

Embryos were isolated from seed pods (siliques) ~140 hr after fertilization. Specifically, expanded siliques were dissected to release developing ovules. Ovules were treated with 5% NaOH to soften the integuments, neutralized in 0.1 M $NaPO_4$, pH 7.0, and placed on glass slides in 50% glycerol and 0.01% Triton X-100. Glass cover slips were pressed onto the ovules by using a watchmaker's forceps to release embryos from the ovules.

Auxin Assays

For measurement of free indole-3-acetic acid (IAA) levels in wild-type and mutant plants, media-grown 9-day-old seedlings were harvested and frozen in liquid nitrogen. Free IAA extractions were conducted as previously described (Carland and McHale, 1996). Samples were assayed by gas chromatography–mass spectrometry as described by Chen et al. (1988).

Auxin transport was assayed in excised inflorescence stems of soil-grown wild-type and mutant plants by using the method of Okada et al. (1991). ^{14}C-IAA was purchased from Sigma.

Mutant strains were tested for altered sensitivity or resistance to auxin (IAA) or to the auxin transport inhibitors 2,3,5-triiodobenzoic acid, 9-hydroxyfluorene-9-carboxylic acid, and *trans*-cinnamic acid (Sigma). Concentrated stock solutions of each compound were prepared in 95% ethanol and added to PNS medium over a range of concentrations. Wild-type and mutant seeds were transferred to the medium, and root lengths were measured after 10 days growth.

Genetic Mapping of *cvp* Mutations

Columbia plants homozygous for each *cvp* mutation were crossed to Landsberg *erecta* strains to generate recombinant F_2 progeny segregating the phenotype of the *cvp* mutants. Homozygous mutant F_2 segregants were identified by their aberrant cotyledon vascular pattern and transferred to soil to be used as a source of DNA for genetic mapping. The map position of each *cvp* mutation was determined by linkage to cleaved amplified polymorphic sequence DNA markers as described elsewhere (Konieczny and Ausubel, 1993).

ACKNOWLEDGMENTS

We are especially grateful for the expert technical assistance of Amy Matsumura, Raymond Ha, and David Tuch. We acknowledge assistance from Evelyn Havir (Connecticut Agricultural Experiment Station) with the free IAA assays. We thank Dr. Thomas Berleth (University of Toronto) for providing mp^{T370} seed. We also thank Drs. Daphne Preuss, Aaron Turkewitz, Celeste Simon (University of Chicago), and Neil McHale (Connecticut Agricultural Experiment Station) for a critical review of the manuscript. This work was supported in part by National Institutes of Health Grant No. GM50408 to B.K. and by U.S. Department of Agriculture Grant No. 96-35-304-3732 and National Science Foundation Grant No. IBN 9808295 to T.N.

Received May 27, 1999; accepted September 6, 1999.

REFERENCES

Aloni, R. (1987). Differentiation of vascular tissues. Annu. Rev. Plant Physiol. **38,** 179–204.

Berleth, T., and Jürgens, G. (1993). The role of the *monopteros* gene in organising the basal body region of the *Arabidopsis* embryo. Development **118,** 575–587.

Candela, H., Marinnez-Laborda, A., and Micol, J.L. (1999). Venation pattern formation in *Arabidopsis thaliana* vegetative leaves. Dev. Biol. **205,** 205–216.

Carland, F.M., and McHale, N.A. (1996). *LOP1*: A gene involved in auxin transport and vascular patterning in *Arabidopsis.* Development **122,** 1811–1819.

Chen, K.H., Miller, A.N., Patterson, G.W., and Cohen, J.D. (1988). A rapid and simple procedure for purification of indole-3-acetic acid prior to GC-SIM-MS analysis. Plant Physiol. **86,** 822–825.

Chen, R., Hilson, P., Sedbrook, J., Rosen, E., Caspar, T., and Masson, P. (1998). The *Arabidopsis thaliana AGRAVITROPIC1* gene encodes a component of the polar-auxin-transport efflux carrier. Proc. Natl. Acad. Sci. USA **95,** 15112–15117.

Dawe, K., and Freeling, M. (1991). Cell lineage and its consequences in higher plants. Plant J. **1,** 3–8.

Dharmawardhana, D.P., Ellis, B.E., and Carlson, J.E. (1992). Characterization of vascular lignification in *Arabidopsis thaliana.* Can. J. Bot. **70,** 2238–2244.

Esau, K. (1965). Vascular Differentiation in Plants. (New York: Holt, Rinehart, and Winston).

Estelle, M.A., and Somerville, C.R. (1986). The mutants of *Arabidopsis.* Trends Genet. **2,** 89–93.

Estelle, M.A., and Somerville, C.R. (1987). Auxin-resistant mutants of *Arabidopsis thaliana* with an altered morphology. Mol. Gen. Genet. **206,** 200–206.

Fukuda, H. (1992). Tracheary element formation as a model system of cell differentiation. Int. Rev. Cytol. **136,** 289–332.

Gälweiler, L., Guan, C., Müller, A., Wisman, E., Mendgen, K., Yephremov, A., and Palme, K. (1998). Regulation of polar auxin transport by AtPIN1 in *Arabidopsis* vascular tissue. Science **282,** 2226–2229.

Hardtke, C.S., and Berleth, T. (1998). The *Arabidopsis* gene *MONOPTEROS* encodes a transcription factor mediating embryo axis formation and vascular development. EMBO J. **17,** 1405–1411.

Haughn, G.W., and Somerville, C. (1986). Sulfonylurea-resistant mutants of *Arabidopsis thaliana.* Mol. Gen. Genet. **204,** 430–434.

Jegla, D., and Sussex, I.M. (1989). Cell lineage patterns in the shoot meristem of the embryo in the dry seed. Dev. Biol. **131,** 215–225.

Kim, J., Harter, K., and Theologis, A. (1997). Protein–protein interactions among the Aux/IAA proteins. Proc. Natl. Acad. Sci. USA **94,** 11786–11791.

Kinsman, E.A., and Pyke, K.A. (1998). Bundle sheath cells and cell-specific plastid development in *Arabidopsis* leaves. Development **125,** 1815–1822.

Klee, H.J., Horsch, R.B., Hinchee, M.A., Hein, M.B., and Hoffman, N.L. (1987). The effects of overproduction of two *Agrobacterium tumefaciens* T-DNA auxin biosynthetic gene products in transgenic petunia plants. Genes Dev. **1,** 86–96.

Konieczny, A., and Ausubel, F.M. (1993). A procedure for mapping *Arabidopsis* mutations using co-dominant ecotype-specific PCR-based markers. Plant J. **4,** 403–410.

Last, R.L., Bissinger, P.H., Mahoney, D.J., Radwanski, E.R., and Fink, G.R. (1991). Tryptophan mutants in *Arabidopsis*: The consequences of duplicated tryptophan synthase β genes. Plant Cell **3,** 345–358.

Lincoln, D., Britton, J.H., and Estelle, M. (1990). Growth and development of the *axr1* mutants of *Arabidopsis.* Plant Cell **2,** 1071–1080.

Luschnig, C., Gaxiola, R., Grisafi, P., and Fink, G. (1998). EIR1, a root-specific protein involved in auxin transport, is required for gravitropism in *Arabidopsis thaliana.* Genes Dev. **12,** 2175–2187.

Mayer, U., Torres-Ruiz, R.A., Berleth, T., Misera, S., and Jürgens, G. (1991). Mutations affecting body organization in the *Arabidopsis* embryo. Nature **353,** 402–407.

Müller, A., Guan, C., Gälweiler, L., Tanzler, P., Huijser, P., Marchant, A., Parry, G., Bennett, M., Wisman, E., and Palme, K. (1998). *AtPIN2* defines a locus of *Arabidopsis* for root gravitropism control. EMBO J. **17,** 6903–6911.

Nelson, T., and Dengler, N. (1997). Leaf vascular pattern formation. Plant Cell **9,** 1121–1135.

Normanly, J., Cohen, J., and Fink, G.R. (1993). *Arabidopsis thaliana* auxotrophs reveal a tryptophan-independent biosynthetic pathway for IAA. Proc. Natl. Acad. Sci. USA **90,** 10355–10359.

Northcote, D.H. (1995). Aspects of vascular tissue differentiation in plants: Parameters that may be used to monitor the process. Int. J. Plant Sci. **156,** 345–356.

Okada, K., Ueda, J., Komaki, M., Bell, C., and Shimura, Y. (1991). Requirement of the auxin polar transport system in early stages of *Arabidopsis* floral bud formation. Plant Cell **3,** 677–684.

Poethig, R.S., Coe, E.H., and Johri, M.M. (1986). Cell lineage patterns in maize embryogenesis: A clonal analysis. Dev. Biol. **117,** 392–404.

Przemeck, G.K.H., Mattsson, J., Hardtke, C.S., Sung, Z.R., and Berleth, T. (1996). Studies on the role of the *Arabidopsis* gene *MONOPTEROS* in vascular development and plant cell axialization. Planta **200,** 229–237.

Raven, P.H., Evert, R.F., and Curtis, H. (1976). Biology of Plants. (New York: Worth Publishers).

Romano, C.P., Hein, M.G., and Klee, H.J. (1991). Inactivation of auxin in tobacco transformed with the indoleacetic acid-lysine synthetase gene of *Pseudomonas savastanoi.* Genes Dev. **5,** 438–446.

Rubery, P.H. (1987). Auxin transport. In Plant Hormones and Their Role in Plant Growth and Development, P.J. Davies, ed (Dordrecht, The Netherlands: Martinus Nijhoff), pp. 341–362.

Sachs, T. (1991a). Pattern Formation in Plant Tissues. (Cambridge, UK: Cambridge University Press).

Sachs, T. (1991b). Cell polarity and tissue patterning in plants. Development **1** (suppl.), 83–93.

Sessions, R.A., Nemhauser, J.L., McColl, A., Roe, J.L., Feldmann, K.A., and Zambryski, P.C. (1998). *ETTIN* patterns the *Arabidopsis* floral meristem and reproductive organs. Development **124,** 4481–4491.

Steeves, T.A., and Sussex, I.M. (1989). Patterns in Plant Development. (Cambridge, UK: Cambridge University Press).

Telfer, A., and Poethig, R.S. (1994). Leaf development in Arabidopsis. In *Arabidopsis,* E.M. Meyerowitz and C.R. Somerville, eds (Cold Spring Harbor, NY: Cold Spring Harbor Laboratory Press), pp. 379–401.

Timpte, C., Wilson, A.K., and Estelle, M. (1994). The *axr2-1* mutation of *Arabidopsis thaliana* is a gain-of-function mutation that disrupts an early step in auxin response. Genetics **138,** 1239–1249.

Tsukaya, H., Tsuge, T., and Uchimiya, H. (1994). The cotyledon: A superior system for studies of leaf development. Planta **195,** 309–312.

Ulmasov, T., Hagen, G., and Guilfoyle, T.J. (1997). ARF1, a transcription factor that binds to auxin response elements. Science **276,** 1865–1868.